

Coating Materials for an Absolute Electron Energy Analyzer (CMA)

W. Y. Li ^a, K. Goto ^{a*}, J. Takioto ^a, S. Tanaka ^a, H. Morikawa ^a and R. Shimizu ^b
^a Nagoya Institute of Technology, Gokiso-cho, showa-ku, Nagoya 466-8555, Japan.
^b Osaka Institute of Technology, Kitayama 1-79, Hirakato 573-0196, Japan.
* goto.keisuke@nitech.ac.jp

(Received: August 20, 2004 ; Accepted: October 25, 2004)

We have been constructing a well defined Auger electron analyzer (cylindrical mirror analyzer; CMA) for standardization which shall need a surface of stable work function in the electron analyzer. To find a suitable material, we measured the work function of carbons (soots, aquadag, graphite, glassy carbon, activated carbon, carbon black, C₆₀, C₇₀ and CNTs) and Au, which have been believed stable. Typical metals Cu(100) and Al were also examined. Experiments were performed in a special PEEM (Photoelectron Emission Microscope) with photoelectric emission method. Work function of the soot (amorphous carbon) aquadag[®] were superior in any conditions of vacuum and the irradiation of UVs but were changed by the ion bombardment of Ar⁺ (1KeV) by -0.29—+0.24eV. The soots and aquadag[®] were found to be the most suitable material for the coating of the electron analyzer.

1. Introduction

Auger electron spectroscopy (AES) and X-ray photoelectron spectroscopy (XPS) are popular in surface analysis and the metrological standards for their calibration references (energy and intensity) have been published as ISO15472 for XPS [1] and ISO 17974 for high resolution AES [2]. About the intensity, three papers were published: Quantitative AES and XPS [3], and determination of the electron spectrometer transmission function and the detector sensitivity energy dependencies for the production of true electron emission spectra in AES and XPS [4]. Standard Reference Spectra for XPS and AES: Their derivation, validation and use, and [5] was a System for the Intensity calibration of electron spectrometers. In addition, NPL has supplied software [6], to provide a traceable calibration of the intensity scales of AES. This calibration is available for the energy range 20 eV to 2500 eV which covers the energy range required for quantitative AES analysis. These works by NPL should be appreciated.

We have been studying another absolute AES for the medium energy resolution, which measures the whole energy range of 1eV to 5000 eV and the range is advantageous to the theory and simulation. We have obtained a log-log plot that covers the whole range of energy distribution including Auger spectra in one sheet is shown in Fig.1. The

scatter in the lower energy range of around 1 eV, true secondary electrons, would mainly be caused by the difference in the work function of each sample with that of the analyzer. It should be needed to adjust/compensate the work function of each sample to the analyzer to obtain a true kinetic energy that based on the “0” vacuum potential energy. The difference of work function shall shift not only the secondary electrons, but also the whole spectrum.

In an actual experiment, we usually pay no attention for the work functions, then an ambiguous value will be resulted in the spectrum. It is a quite common problem in AES and any other energy analyses as well. To obtain a reference spectrum to calibrate the analyzer and to offer the standard [7], we have to find the method to correct the work functions of the analyzer (CMA). An iterative method for the analyzer [8] and the observation of an energy distribution of the secondary electrons have been examined: The former was successful for 40-1200 eV with 15 meV of accuracy and the latter showed feasibility [9]. A PC simulation was also employed to determine a configuration around the sample to correct the work function difference of the analyzer and the sample by calculating the electron orbit to the CMA. According to the simulation, an optimum configuration was determined [10]. Now we need a stable surface in the electron analyzer even for the frequent introduc-

tion of air and gases, any vacuum, bombardment of electrons, ions and energetic neutrals, which shall be required for the absolute AES for its standardization. Low secondary electron yield is also required for the material in the coating of the analyzer to reduce the electron scattering, which would result in a superior signal to noise ratio in the spectra. It has been believed that carbons are the most stable material. Many figures and properties have been reported about them [11, 12]. It is interesting how atomic scales of structure would present macroscopic characteristics of work function. Our main concern is the work function, *i.e.*, contact potential difference and the secondary electron yield.

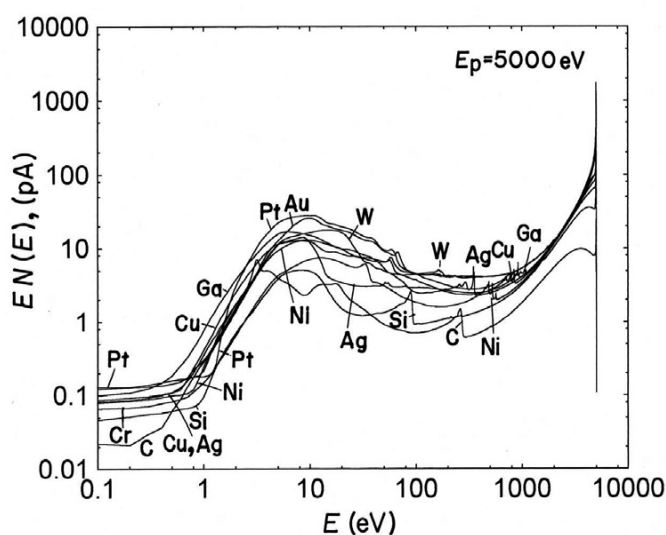


Fig. 1. Typical spectra in log-log plot for typical samples. Intensity was normalized to primary current of 1 μ A.

Presently, soot aggregates (amorphous carbon) and aquadag[®] are the most suitable candidate and it has been satisfactorily used in our laboratory. It is said that the other figures of carbons, *i.e.*, graphite, glassy carbon, activated carbon, carbon black, fullerenes, CNTs, aquadag[®] etc., are also stable in any environments. Though the stability for ion irradiation is not clear and will be examined in this paper. These materials were measured in an absolute method, by photometric, *i.e.*, a method in a special PEEM (photoemission electron microscope) being modified from the commercial PEEM of Staib Instrument Model 350 [13]. This measurement method is very sensitivity and has superior space selection property.

It was found in our experiments that the soot (amorphous carbon) and aquadag[®] can be the most suitable candidate and have durable features for coating in the CMA. This may

come from the fractal-like complex “coral” structure. In addition, the secondary electron yield is one of the lowest (broad yield of $\delta=0.30-0.50$ for primary electron energies 200-700 eV, correspondingly, and it increased to be about 0.7 being settled in alcohol suspension by the agglomeration) among the materials [14]. It is also stable for an electron beam bombardment (300 V, 1 mA/cm²) [15].

2. Experimental

The schematic PEEM system is shown in Fig.2. We have modified the commercial PEEM for the particular measurement of work function. Thus the PEEM was operated in a lower magnification of about 10 being the optimum to get the maximum intensity. Monochromatized UVs, by using a D₂ lamp and a monochromator (Jobin Yvon, H-UV20), were irradiated over the sample and the sample area observed by the PEEM was approximately 1 mm in diameter. The incident angle was 60° from the surface normal. Emitted photoelectrons were detected by a simple electronic counting method, which we contrived [16]. The monochromator was calibrated by using a Hg-lamp. The resulting photoelectrons are projected on the screen of the PEEM as spots. The vacuum chamber can evacuate below 10⁻⁸ Pa, and the main residual gases were H₂ and CO which might be adsorbed on the sample. The sample was sputtered by Ar⁺ of 250-1000 eV incident at 60° from the surface normal with sample rotation. The background (electronic noises and the natural radiations) of the PEEM system on the absence of UVs was measured from 0.1 to 0.4 cps. The spots can be counted by electronic system as well as manually by eye. The use of the PEEM shows advantages of spatial selectivity and sensitivity. In the work function measurements the signal to noise ratio is a predominant term to determine the value of work function, because we measure the threshold of the photoelectron yield by the intersection of the yield and noise (background). Our photoelectron counting method showed an ultimate sensitivity. To determine the work function by the threshold would include some ambiguities for the true value. One is the broadening of the Fermi edge at the room temperature of the experiments. Hence, a PC simulation of the threshold method was studied [17].

The samples used in the experiments were commercially available ones except the soots. The soots were made by burning a fuel butane gas, liquid benzene, solid naphthalene in the air and directly coated on the sample holder in the flame.

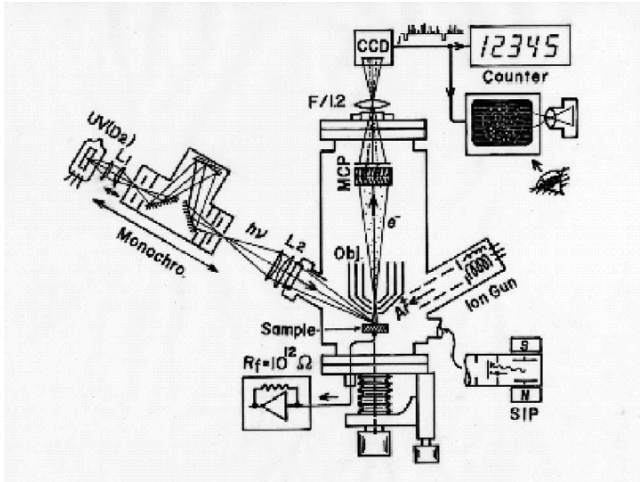


Fig.2. Schematic PEEM system.

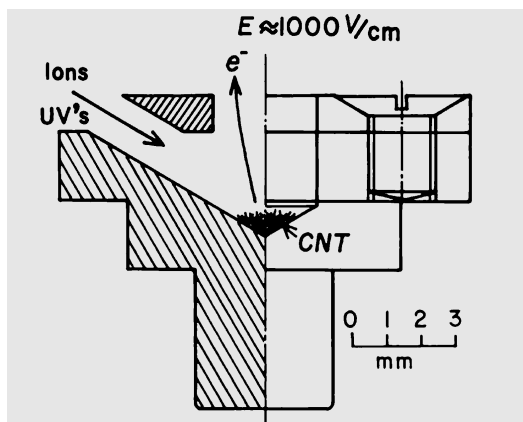


Fig.3. Sample holder for CNT. The electric field at the sample can be reduced by a factor of 58. UVs and ions can irradiate the sample through the side hole.

In the experiments, a special care must be paid for the field emission (FE) of single-walled carbon nanotubes (CNTs), which could be easily yielded even in the extraction field of the PEEM electric field of lower than 1000 V/cm, the common flat table sample holder cannot be used. We made a special sample holder shown in Fig.3. The sample was put at the bottom of hole, for which the electric field was effectively reduced. The UV lights and ions can irradiate the sample through a hole beside the holder at 60° for the axis of the holder. We did a PC simulation of the electric field around the hole, and reduced electric field by a factor of 58 can be obtained at the bottom area. The extraction field being inherent to PEEM was effectively shielded for the sharp-shaped samples. While the lens ef-

fect of the holder and objective lens should distort the PEEM image, which may be useless as the observation of the surface structure. The FE from the CNTs was so decreased that the work function of CNTs was measured.

On the other hand, to find the cause that would yield the difference of the work function, the shape and structure of the soots as evacuated and after ion sputtering (Ar^+ , 250-1000 eV), were observed by a transmission electron microscope (TEM; JEM-2010). The structures of the fullerenes as received and after ion bombardment were observed by a scanning electron microscope (FE-SEM; Hitachi 5700S).

3. Results and discussion

The structure of soot which was made from a butane flame, was observed by the TEM. The TEM images of the soot of butane aggregate are shown in Fig.4. The surface structure of soot is so rough. Typical soot was of open-structured aggregate of small particles in which a small flake like lamination (graphite?) can be seen like a coral and each particle had nearly similar shape and diameter of about 20 nm (left) with poor contrast. Fig.4 (right) shows the ion (Ar^+ , 250 eV) bombarded soot, the structure seems to be quite as same as that of before ion sputtering but with somewhat better contrast. The threshold characteristics of the soot as received and after ion sputtering are shown in Fig.5, the cross being assumed to be the threshold, and the series of experiments were averaged and determined to be 4.41(4) eV and 4.40(3) eV after saturation with enough sputtering of more than 10 atomic layers, respectively. The errors (uncertainty) in standard deviation in parentheses were estimated considering the energy resolution of the monochromator and experimental standard deviation. The difference of 0.01 eV was very small as within the standard deviation, and it can be said that the work function in this particular case did not practically change even after the ion sputtering. Another experiments showed similar characteristics of as evacuated condition and with mild ion sputtering of 250 eV, however, the value of 4.76(4) eV after the 1000 eV of Ar^+ sputtering. In the start of the ion sputtering it always showed the smallest work function of about 4.34 (min.) eV, then after changed. We should think that the ion sputtering would alter the work function due to the structural change of the specimen. This phenomenon shall inevitably be the general feature.

A soot made from a benzene flame is called as "wooly" soot and has been used as the best absorber for electrons

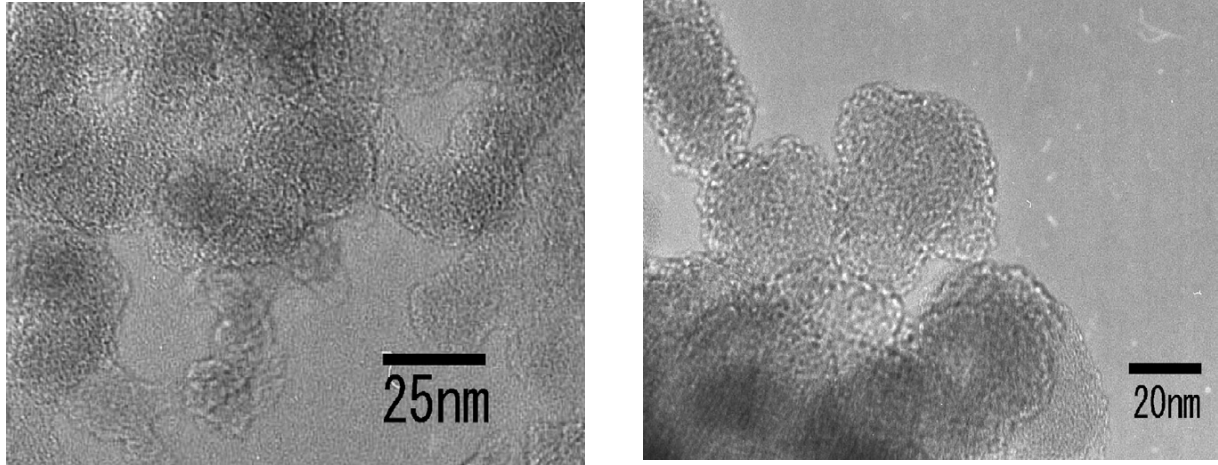


Fig.4. The TEM images of the soot aggregate made from butane gas. The structure of soot as received (left) and after ion (Ar^+ , 250 eV) bombardment (right).

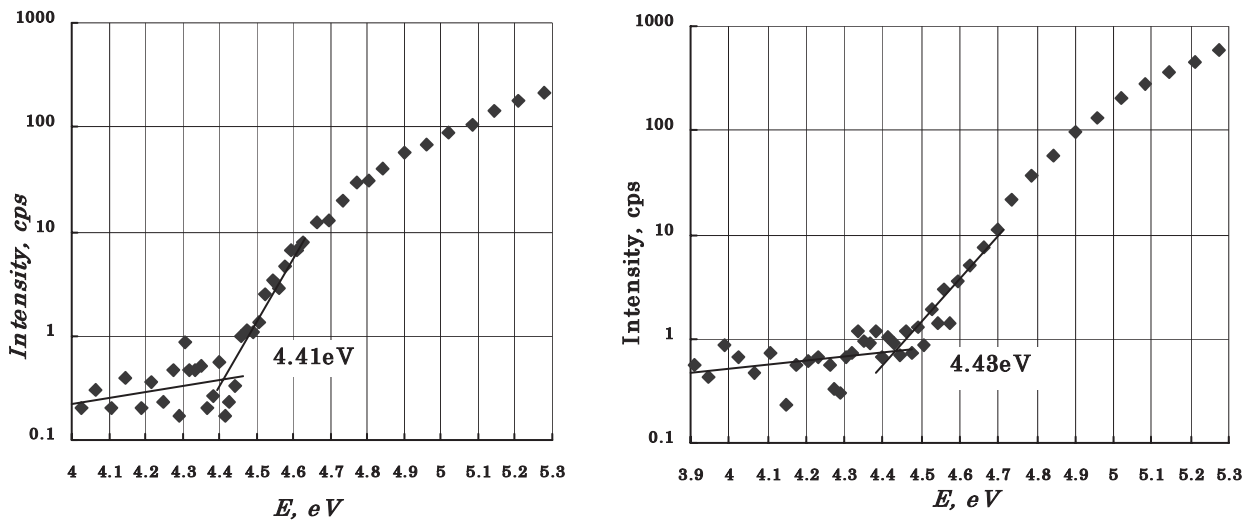


Fig.5. Threshold (at the cross) of soot as received (left) and after ion sputtering (right). The threshold (the work functions) of the soot was determined to be 4.41 eV and 4.43 eV.

and photons. It is, however, rather bulky and would get thickness. The work functions of soot made from benzene being determined similarly as in the butane before and after ion sputtering were 4.53(4) and 4.45(4), respectively. The difference of 0.08 eV was considerably larger than that of butane gas (0.02 eV), so it was not better than the soot made from butane flame, but can be used for the CMA. The structure of the soot was observed by TEM and it was shown in Fig.6. It was also like a complex coral having open-structured geometry and the agglomeration of diameter of about 20 nm of block. Many balls (about 0.5 nm) were seen in it. After ion sputtering, the wall of open-structured geometry was torn a little and the smooth peripheral wall became to

be rough, but the internal structure was not likely changed. This small change might cause the work function change.

Naphthalene the main constituent of popular camphor is also a good soot material. The work functions of soot made of naphthalene, before and after ion sputtering, were measured to be 4.85(5) eV and 4.55(5) eV (4.74 eV at the beginning), respectively. After ion sputtering, to estimate the effect due to the residual gas, the soot was held in the vacuum chamber (low of 10^{-8} Pa) about 120 hours, then the work function was decreased to be 4.50 eV. The difference before and after the adsorption was 0.25 eV and this was considerably large for the CMA use.

The soot consists of some variety of crystals. The fractal-

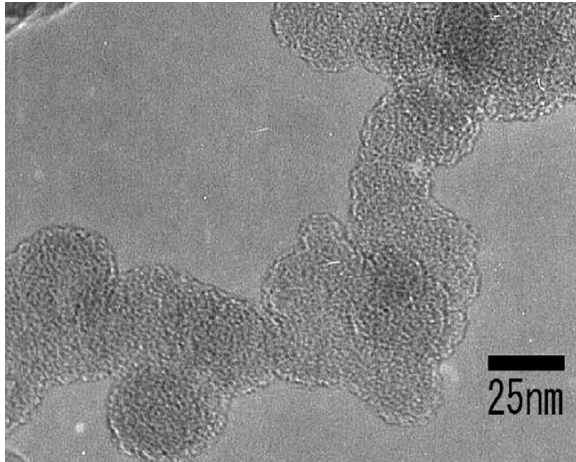


Fig.6. The TEM image of the soot aggregate made from benzene, after ion (Ar^+ , 250 eV) bombardment.

like and projected aggregate structure properties would give to be durable characteristics that are relatively independent of fuel type and flame conditions [18]. In addition to this property the low secondary electron yield characteristic should be emphasized for the use in an energy analyzer, because of which surface can not be retouched after the construction of an analyzer. The soot is a good conductor and also has durable property. Thus, we can say that the soot is the most suitable material that we have ever experienced.

The work functions of aquadag® (Hitachi, AB-1 for vacuum tubes) before and after ion sputtering were 4.65(5) eV and 4.73(7) eV (4.57 eV at the beginning), respectively. The difference was 0.08 eV and it seemed also suitable material. The ion sputtered aquadag was held in the vacuum chamber (low of 10^{-8} Pa) about 72 hours, and 4.61 eV was resulted. After that, the sample was taken out once in the air, then putted it into the vacuum chamber again, and the threshold was 4.78 eV. It seemed good material, though we should confirm the stability more carefully as it consists of complex materials.

The work function of the highly oriented pyrolytic graphite (HOPG) as received was 4.73(4) eV and agreed with the reported values (4.8 eV [19], 4.6 eV [20]). It has been changed from 4.37 to 4.63 eV after the ion bombardment, simultaneously the surface of “graphite” structure was broken. In consequence, the electronic structure was altered and accordingly the work function.

The work function of the as received glassy carbon was 4.92(5) eV and it reduced with ion sputtering from 4.61 (at

the beginning) to 4.34 eV (saturated). The surface of structure might be broken by the ions as well.

The work function of the charcoal activated was 4.58(8) eV (as received) and after ion sputtering it changed from 4.67 to 4.82(5) eV being not stable.

The work function of the as received carbon black for the industrial use was 4.89(4) eV and after ion sputtering it became 4.74 (at the beginning) \sim 4.67(7) eV, being not stable also.

Recently fullerenes and carbon nanotubes have been extensively studied for their unique properties. It is said that these carbon materials are stable for any conditions. Thus we studied some of these in the same manner as in the former soots and carbons. The threshold (ionization potentials) of C_{60} as received and after ion sputtering were 6.16 eV and 5.65 \sim 6.12 eV, respectively. The values were, however, lower than the reported (7.61 eV) [21]. The results were remarkably higher than those of conductor materials (about 4 eV \sim 5 eV). Because it is a special atomic structure of crystal, the binding force of electron is strong, so that the higher value can be considered. The threshold of C_{70} (ionization potentials) as received and after ion sputtering were 4.75 and 4.49 \sim 4.80 eV, respectively. The structure of fullerenes might be torn by the ion bombardment and change the crystals. Figs.7 and 8 show the change of crystals of C_{60} and C_{70} being observed by an FE-SEM. Some agglomeration and polymerization-like features were observed but we have not understood yet. Because various surfaces were oriented, the corresponding the threshold should be different. The resulting the threshold may be a certain average. The ion sputtered C_{60} was held in the vacuum in the low range of 10^{-8} Pa for about 72 h and was observed by PEEM with UVs of about 5.4 eV, without exit slit of the monochromator to enhance the signal and a series of the display for 40 s is shown in Fig.9. The change ceased at the end of the period and saturated for the further irradiation. Correspondingly, the threshold was changed as well. This might be due to desorption of the adsorbed gases, hydrogen the main residual element we guess by the UV's, because the torn structure would easily adsorb the residual gases. In the literature the H_2 dissociative adsorption at the edges of graphite for C_{60} was reported [22]. Fullerene is a kind of insulating material and it would charge up, but the change in Fig.7 can not be considered as a result of charge up because the photoelectric current was so small as 10^{-16} A or below.

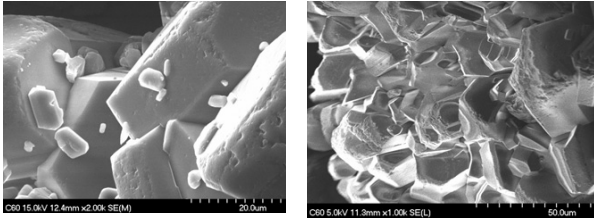


Fig.7. The structure of C_{60} as received (left) and after ion (Ar^+ , 250 eV) bombardment (right).

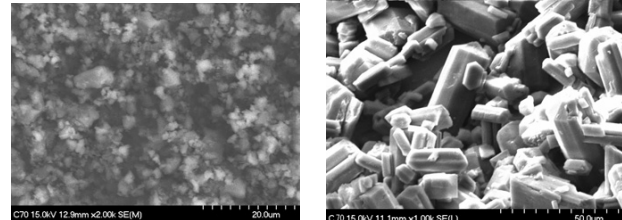


Fig.8. The structure of C_{70} as received (left) and after ion (Ar^+ , 250 eV) bombardment (right).

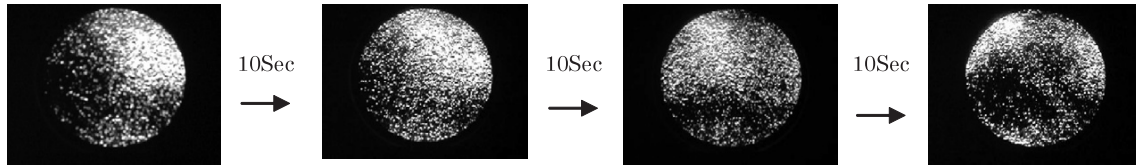


Fig.9. The ion sputtered C_{60} was observed by PEEM *i.e.*, irradiation of UVs of about 5.4 eV.

The work function of carbon nanotubes (CNTs) were ranging from 4.2 to 4.4 eV and lower than the report (4.63 ~ 4.77 eV) calculated with first-principles [23]. The work function and geometrical structure directly influence the field emission (FE) properties. In the experiments, a field emission of CNTs was easily yielded and it can be observed in the display of the PEEM. This was quite natural because the CNT is a sharp needle. The FE was unstable in as received state but quite stable after ion bombardment. This might be due to the adsorption and desorption of the contaminations. The FE of the ion sputter cleaned CNTs showed little changes for 10 hours or more. It was found that the clean CNT was an excellent electron source. The work function and shape of the material are crucial to understand the FE properties.

The characteristics of carbons should be compared with those of Au as it has been used as a reference material, Cu and Al as conventional base materials. The work functions of Au (100), (110), (111), and poly crystals, were measured in the same PEEM to be 5.08(4), 5.04(5), 5.12(6), and 4.80(11) eV, respectively. The as received AUs would have tendency to show lower work function than the pure ones. This might be due to the adsorbed contaminations. Though the continuous (several runs) experiments would gradually reveal the characteristics of clean ones by the UV enhanced desorption. The work function of Au has not changed after the ion bombardment in the UHV. So Au will be unstable in vacuum, storing conditions, irradiation of ions and UVs. It

can be said that metals are not stable but would be saturated after ion sputtering such as Au (100), Au (110) and Au (111), it is not suitable as the coating material for CMA. While Au has been used in some analyzers and Kelvin probes in vacuum and atmosphere [24, 25], we found it is also unsuitable in these applications as a reference material.

Incidentally Cu (100) and Al (111), (100), (110) were measured in the same way. It was quite natural that the reactive metals like Als should quickly adsorb the residual gases even in UHV and continued to change the work function after the sputter cleaning. These metals were not so stable as a coating material as we would expect. Sometimes metals showed a broad and dull threshold.

The obtained results are tabulated in Table 1. It was found, the carbon materials in comparison with Au, Cu, and Al show variety of characteristics; the value of work function and stability for the argon ion sputtering. We see reference values of work function : Fomenko [26] gave recommended values (individual value scattered too much) for C, Al, Cu, and Au as to be 4.7 eV, 4.25 eV, 4.4 eV, and 4.3 eV, respectively, and Michaelson [27] correspondingly gave the values 5.0 eV, 4.28 eV, 4.65 eV, and 5.1 eV.

Table 1. Experimentally obtained work functions.

	As evacuated (eV)	After ion Sputtering (250-1000 eV)	Comments
soot (butane)	4.41(4)	4.34 → 4.40(3)/4.76(4)	Superior but being altered by ion sputtering of 1000 eV
soot (benzene)	4.53(4)	4.47 → 4.45(4)	Superior but rather bulky (wooly)
Soot (naphthalene)	4.85(5)	4.74 → 4.55(5)	stable but considerable change after ion sputtering
aquadag®	4.65(5)	4.57 → 4.73(7)	stable but the secondary electron yield is higher than soots
graphite	4.73(4)	4.37 → 4.63	stable but torn by ions
glassy carbon	4.92(5)	4.61 → 4.34(5)	stable but torn by ions
charcoal activated	4.58(8)	4.67 → 4.82(5)	not stable
carbon black	4.89(4)	4.62 ~ 4.75	not stable
C ₆₀	6.16	5.65 ~ 6.12	stable but broken and agglomerated by the ions
C ₇₀	4.75	4.49 ~ 4.80	visual size of the piece scattered away from the sample holder
CNT	4.35 ~ 4.77	4.2 ~ 4.4	difficult to prepare and easily emits FE
Au (100)	4.48 → 5.05	5.08(4)	as evacuated surfaces were not stable but would be saturated and stable in the vacuum after UVs irradiation and ion sputtering, adsorbed residual gases for a day of exposure in UHV
Au (110)	4.54 → 4.97	5.04(5)	
Au (111)	4.67 → 5.12	5.12(6)	
Au(poly)	~ 4.83	4.62 → 4.80(11)	
Cu(100)	4.76	4.81 → 4.24 (11)	unstable even in UHV
Al(111)	3.57	4.10 → 3.90/200 min	changed in minutes in UHV and other Al(100), (110) changed similarly.

4. Summary

From these experimental results, the work function of soots that made from butane gas, benzene, and naphthalene, and that of aquadag® did not practically change as long as in as received and UV irradiation in UHV, but showed some change of characteristics that amounted to be 0.4 eV at most with Ar ion sputterings (250-1000 eV). This can be said quantitatively that it would come from a kind of 'Fractal-like' structures. The soots and aquadag® are suitable candidate and have been satisfactorily used in our CMA. Though for the complex material of aquadag®, we should need further confirmation. It can be applicable to other electron analyzers and apparatus. The secondary electron yield of the aquadag® is 0.75 [15] and the value is rather higher than the soots. The structure of the soot depends on the materials and correspondingly the work functions. Some perceptible geometrical shape on the ion sputtering was

observed by the TEM. In the critical study, such as metrological measurements, the coating shall not be exposed to the ions and energetic neutrals. The latter can also sputter the surface and change the structure. Our CMA is provided for the ions by shutter between the CMA and ion gun. The graphite and glassy carbon were easily torn by ions. The other carbons of the charcoal activated and carbon black showed similar properties. The changes of the fullerenes were enormous in the geometrical property by ion sputtering. Correspondingly, the work functions were changed. The CNT also showed the changes for the vacuum and ion bombardment, however, the detail was not analyzed because of the nano-fiber structure. As a precious metal would seem to be stable only after the cleaning by UVs irradiation and ion sputtering. We found Au may be unsuitable in Kelvin probes and coating material for CMA applications, further metals such as Al and Cu are of none the unexception.

Acknowledgments

The work has been supported by the Special Coordinated Research of Science and Technology through NRIM (now NIMS). We would like to express our sincere thanks to Dr. P. Staib of Staib company, Dr. Y. Sakai of JEOL, and S. Fujii of our institute for their technical supports, Professor Y. Yashiro for his information. Associate Professor M. Tanemura of NIT for the samples.

References

- [1] M. P. Seah and I. S. Gilmore, *J. Electron Spectrosc. Relat. Phenom.* **83**, 197 (1997).
- [2] M. P. Seah, *J. Electron Spectrosc. Relat. Phenom.* **97**, 235 (1998).
- [3] M. P. Seah and G. C. Smith, *Surf. Interface Anal.* **15**, 751 (1990).
- [4] G. C. Smith and M P Seah, *Surf. Interface Anal.* **16**, 144 (1990).
- [5] M. P. Seah, *J. Electron Spectrosc. Relat. Phenom.* **71**, 191 (1995).
- [6] <http://www.npl.co.uk/nanoanalysis/a1calib.html>.
- [7] K. Goto, Y. Z. Jiang, N. Nissa Rahmen, Y. Asano, and R. Shimizu, *Surf. Interface Anal.* **34**, 211 (2002).
- [8] K. Goto, N. Nissa Rahmen, Y. Z. Jiang, Y. Asano, and R. Shimizu, *Surf. Interface Anal.* **33**, 245 (2002).
- [9] Y. Z. Jiang, W. Y. Li, K. Goto and R. Shimizu, *J. Surf. Anal.* **9**, 348 (2002).
- [10] Y. Z. Jiang, R. Kato, K. Goto and R. Shimizu, *J. Surf. Anal.* **11**, 2 (2004).
- [11] Bruining, H. "Secondary Electron Emission" *Philips Tech. Rev.*, **3**, 80. (1938).
- [12] K. G. Mckay, "Advances in Electronics." **1**, p78 (1948).
- [13] W. Y. Li, K. Goto and R. Shimizu, *Surf. Interface Anal.* (to be published).
- [14] R. O. Jenkins and W. G. Trodden: "Electron and ion emission from solids," London, Routledge and Kegan Paul p63 (1965).
- [15] A. H. Beck : "Handbook of Vacuum Physics," Volume 2 Physical Electronics Parts 2 and 3, Pergamon press, Oxford, New York, London, Edinburgh, Toronto, Paris, Frankfurt, p319 – 327 (1966).
- [16] S. Ichimura, K. Goto, and K. Kokubun, *Rev. Sci. Instrum.* **61**, 1192 (1990).
- [17] W. Y. Li, D. Yamada, K. Goto and R. Shimizu (unpublished).
- [18] Ü. Köylü and G. M. Faeth, *Combustion and Flame* **100**, 621 (1995).
- [19] M. Shiraishi, M. Ata, *Carbon* **39**, 1913 (2001).
- [20] S. Suzuki, C. Bower, Y. Watanabe, and O. Zhou, *Appl. Phys. Rev. Lett.* **82**, 2548 (1999).
- [21] J. A. Zimmerman, J. R. Eyler, S. B. H. Bach, and S. W. McElvany, *J. Chem. Phys.* **94**, 3556 (1991).
- [22] W. A. Dino, H. Nakanishi, H. Kasai, T. Sugimoto, and T. Kondo, *Surf. Sci. Nanotech.* **2**, 77 (2004).
- [23] Zhao, J. Han, and J. P. Lu, *Phys. Rev.* **B65**, 193401 (2002).
- [24] Lord Kelvin, *Phil. Mag.* **46**, 82 (1898).
- [25] W. A. Zisman, *Rev. Sci. Instrum.* **3**, 367 (1932).
- [26] V. S. Fomenko, "Hand Book of Thermionic Properties" Plenum Press Data Division (1966).
- [27] H. B. Michaelson, *J. Appl. Phys.* **48**, 4729 (1977).